Microfluidic production of polyacrylic acid functionalized PEG microgels for efficient biomolecular conjugation

Yoon Choi[1], Su-Ryeon Park[1], Sei-Jung Lee[2] and Chang-Hyung Choi[1]*

[1]Division of Cosmetic Science and Technology, Daegu Haany University, Gyeongsan-si, Gyeongsangbuk-do, South Korea, [2]Department of Pharmaceutical Engineering, Daegu Haany University, Gyeongsan-si, Gyeongsangbuk-do, South Korea

We present a double emulsion drop-based microfluidic approach to produce uniform polyacrylic acid functionalized polyethylene glycol (PAA-PEG) microgels. By utilizing double emulsion drops as templates, we produce monodisperse microgels by rapid photopolymerization of the inner prepolymer drop consisting of polyacrylic acid (PAA) and polyethylene glycol diacrylate (PEGDA), followed by dewetting the oil layer when they disperse into an aqueous media. The size control of the PAA-PEG microgels with a broad range is achieved by tuning the flow rate of each phase; the uniformity of the microgels is maintained even when the flow rate changes. The results show rapid R-phycoerythrin (R-PE) coupling with the microgels' carboxylate with minimal non-specific adsorption, demonstrating highly efficient and reliable biomolecular conjugation within PAA-PEG microgels.

Introduction

Microgels offer significant utility in widespread applications including biosensing, (Li et al., 2018; Li et al., 2020) drug delivery, (Abdelaziz et al., 2018; Liang et al., 2019) catalytic support, (Hwang and Lee, 2019; Hakala et al., 2020; Steinacher et al., 2021) and tissue engineering (Riley et al., 2019; Daly et al., 2020; Hakala et al., 2020). Recent advances in microfabrication techniques enables simple yet reliable manufacturing of microgels with controllable physicochemical properties (Wang et al., 2014; Jo and Lee, 2020). For instance, micromolding and photolithography-based techniques produce functional microgels with tunable size, shape, and chemical compositions (Dendukuri et al., 2006; Choi et al., 2012; Liu et al., 2016; Qu et al., 2019). Microfluidic technique is an alternative route to allow continuous production of microgels with controllable size and compartment by simply tuning of multiphasic flow (Dendukuri and Doyle, 2009; Yadavali et al., 2018). Also, the incorporation of biomolecules or cells within the microgel's network is readily achieved by taking advantage of microfluidics, enabling the development of

versatile techniques for multiplexed suspension arrays for biosensing or tissue engineering applications (Leng et al., 2015; Lee et al., 2019). While technical advances have emerged, there still exists an unmet need for consistent production of functional microgels with uniformity in chemical compositions. Especially, there are many reports of uniform microgels holding various functions (e.g., magnetic, encoding, or encapsulation of biomolecules), there is a lack of technique to impart functionality in a simple, reliable, and efficient manner. In addition, while the batch based micromolding technique provides reliable routes to uniform and chemically functional microgels, the production rate is relatively low. Incorporating chemical functionalities into microgels in a rapid and efficient microfluidic fabrication method would thus represent a significant step forward by utilizing simple post-functionalization with biomolecules.

Our approach to address these technical limitations is an integrated fabrication-conjugation route using a microfluidic production of chemically functional hydrogel microgels, followed by efficient chemical reactions for biomolecular conjugation (Jung and Yi, 2012). We have shown that functional microgels with carboxylate have been prepared by incorporating acrylic acid (AA), using water-in-oil-in water (W/O/W) double emulsion-based microfluidic approach (Liu et al., 2016; Liu et al., 2018); this approach enables one-step production of microgels without additional washing steps by the spontaneous dewetting of a sacrificial oil layer when dispersed in water. Although these techniques provide simple and robust production of functional microgels, co-monomer (e.g., acrylic acid) used for microgel functionalization is highly miscible with oil and water, exacerbating uniformity in chemical functionality.

Herein, we demonstrate the production of polyacrylic acid functionalized polyethylene glycol (PAA-PEG) microgel *via* double emulsion-based microfluidic approach. We use double emulsion drop with a thin sacrificial oil layer as templates, producing monodisperse microgels by photopolymerizing the inner core and then spontaneous dewetting of the oil layer as they are dispersed in water. The resulting PAA-PEG microgels are highly uniform in size, and their dimension is readily controlled by the varying flow rate of each phase, while we incorporate viscous PAA to impart carboxyl group within the PEG network. Finally, we use a fluorescent R-phycoerythrin (R-PE) model protein to demonstrate highly efficient and reliable biomolecular conjugation within PAA-PEG microgels.

Materials and methods

Materials

1-ethyl-3-(3-(dimethylamino)propyl) carbodiimide HCl (EDC), Tween 20, and n-Hexadecane (99%) were purchased from Thermo Fisher Scientific (Waltham, MA, United States).

Poly (ethylene glycol) diacrylate (PEGDA, M_n 700 Da), 2-hydroxy-2-methylpropiophenone, acrylic acid, poly (acrylic acid) (average ~4,000,000), poly (vinyl alcohol) (87%–89% hydrolyzed), n-octadecyltrimethoxyl silane, 2-(4-morpholino) ethanesulfonic acid (MES), N-hydroxysuccinimide (NHS), R-phycoerythrin (R-PE), and phosphate buffered saline (10 mM phosphate, 0.0027 M potassium chloride, 0.138 M sodium chloride; pH 7.4) were purchased from Sigma-Aldrich (St. Louis, MO, United States). 2-[Methoxy (polyethyleneoxy) propyl] trimethoxy silane was purchased from Gelest (Morrisville, PA, United States). The glass capillaries were purchased from AIT Glass (Rockaway, NJ, United States).

Device fabrication and generation of double emulsion drops

To prepare injection capillaries with an orifice diameter of 150 μm, we tapered circular glass capillaries (1B100-6, World Precision Instruments, Inc., Sarasota, FL, United States) using a micropipette puller (P-97, Sutter Instrument, Novato, CA, United States). The injection capillaries were dipped into n-octadecyltrimethoxy silane for 5 min to make the capillary wall hydrophobic; these are subsequently rinsed with isopropyl alcohol to remove residual silane. The injection capillary was then put into the square capillary whose inner width (1.05 mm) is matched with that of the outer diameter of the injection capillary. Next, the small-tapered capillary with 50 inner diameter was prepared by hand using an alcohol ramp; this capillary was put into the injection capillary to supply aqueous solution of prepolymer. Next, the collection capillary was put into the square capillary from the opposite end; this capillary is rendered with 2- [methoxy (polyethyleneoxy)propyl] trimethoxy silane to have the capillary wall hydrophilic. For generating double emulsion drop with a thin oil layer, each phase is continuously supplied and precisely controlled by syringe pumps (KD Scientific Inc., LEGATO 100, Holliston, MA, United States). The resulting double emulsion drops and microgels were observed using an inverted microscope (DMi8, Leika, Germany) equipped with a high-speed camera (Photron USA Inc., MINI UX 50, San Diego, CA, United States).

EDC/NHS activation of the microgels

To confer the carboxylate groups of the microgels into reactive NHS ester groups, we added 400 mM EDC and 400 mM NHS into microgel suspension in 20 mM MES buffer (pH 6) containing 0.05% (v/v) Tween 20 at room temperature. To remove unreacted EDC and NHS, we rinsed the microgel suspension with 20 mM MES buffer (pH 6) containing 0.05% (v/v) Tween 20 several times and 10 mM phosphate-buffered saline (pH 7.2).
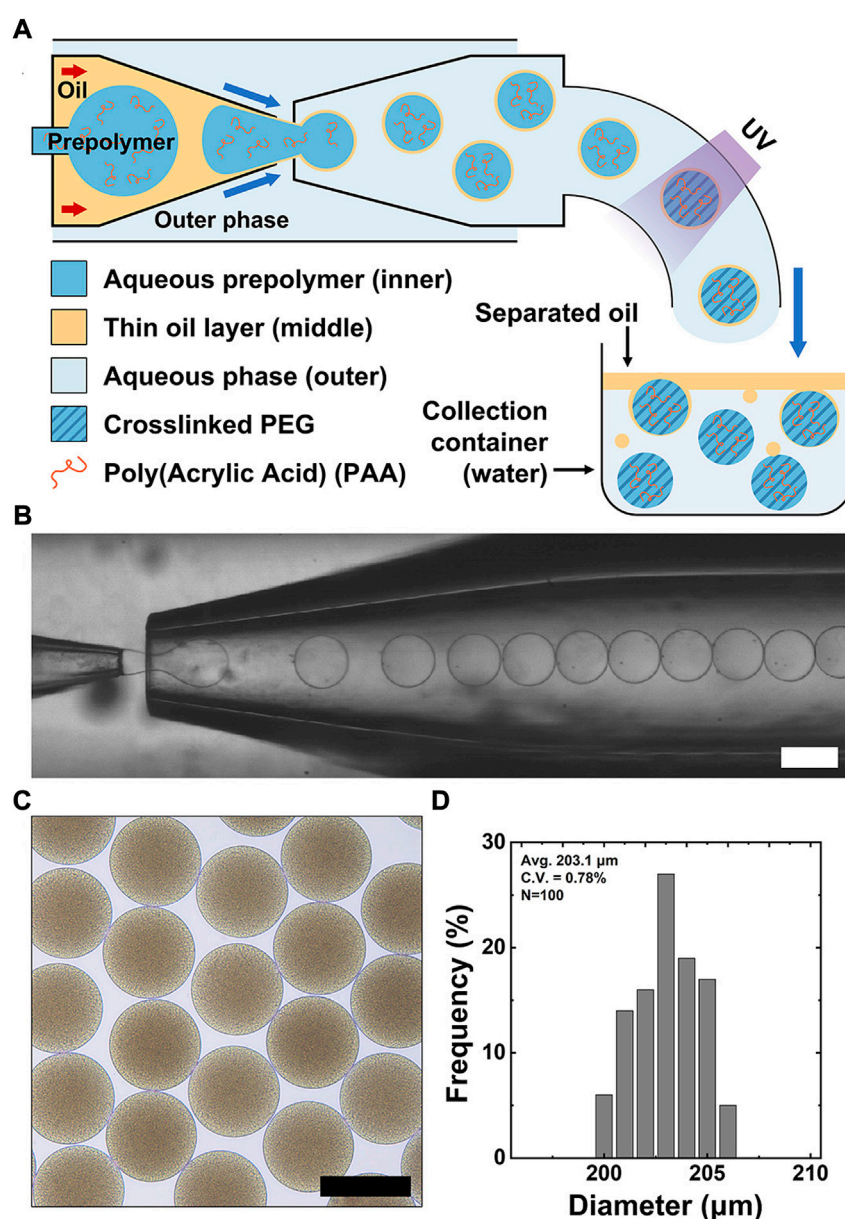
FIGURE 1
Capillary-based microfluidic production of PAA-functionalized PEG (PAA-PEG) microgels using double emulsion drops with a thin oil layer. **(A)** Schematic diagram of the glass capillary microfluidic device used to generate double emulsion drops containing polyethylene glycol diacrylate (PEGDA), PAA, and photoinitiator in the inner drop. These double emulsion drops are polymerized by UV illumination and collected in an aqueous solution to induce the thin oil layer's dewetting from the polymerized microgels. **(B)** Bright-field micrograph showing continuous stream of double emulsion drops. **(C)** Bright-field micrograph showing uniform microgels dispersed in water. **(D)** Size distribution of the resulting microgels C.V. = 0.78%. Scale bars represent 200 μm.

R-phycoerythrin protein conjugation with the microgels

To achieve R-PE conjugation, we added 2 μM R-PE and incubated for up to 24 h into PAA-PEG microgel suspension activated with EDC/NHS on a rotator at room temperature. To remove unreacted R-Pes, we rinsed the microgel suspension several times with 10 mM phosphate-buffered saline (pH 7.2) with 0.05% (v/v) Tween 20. Total fluorescence intensity from the conjugated R-PE is normalized by dividing the intensity at every time-point (I) by the fluorescence intensity of the first time point (I_0).

Results and discussion

We first show capillary microfluidic-based fabrication of polyacrylic acid functionalized PEG (PAA-PEG) microgels using double emulsion drop as templates (Figure 1A). The glass capillary device consists of three circular capillaries with different orifice sizes inserted into a square capillary. The injection and collection capillaries are rendered to provide hydrophobic and hydrophilic surfaces, respectively. Both capillaries are coaxially in the middle of the collection capillary. In addition, a small-tapered circular capillary is inserted into the injection capillary to allow injection of the prepolymer phase. Finally, the collection capillary is connected to polyethylene (PE) microtubing, where ultraviolet (UV) illumination occurs.

To generate double emulsion drops, an aqueous prepolymer solution consisting of polyethyleneglycol diacrylate (PEGDA, 10%), polyvinyl alcohol (PVA, 2%), polyacrylic acid (PAA, 0.2%–1%), and photoinitiator (1%) is supplied through the small tapered capillary to form the inner drop. An oil phase (n-hexadecane with 2% Span80) is supplied through the injection capillary to form a thin oil layer. The coaxial biphasic flow in the injection capillary facilitates the formation of a thin oil layer surrounding the inner prepolymer drop due to the strong wettability of the oil phase to the injection capillary's hydrophobic surface. An aqueous outer phase (5% PVA aqueous solution) is supplied through the interstices between the square and the injection capillaries, while the interstices of the square and circular collection capillaries are sealed, which allows the emulsion stream to flow through the collection capillary. The coaxial flow (water-in-oil) from the injection capillary breaks up into drops by shearing of the aqueous outer phase near the injection capillary's entrance, resulting in monodisperse double emulsion drops with a thin oil layer. These emulsion drops are then exposed to UV illumination (23W/cm², exposure time: 3 s) at the end of polyethylene tubing (15 cm) inserted into the collection capillary, forming PAA-PEG microgels coated with the oil layer in a consistent manner. When they are suspended in aqueous solution of the collection container, the oil layers separate from the microgel's surfaces by dewetting process, leaving PAA-PEG microgels; the separated oil drops move toward the top surface due to the lower density of hexadecane oil ($\rho_{hexadecane}$ = 0.77 g/ml) than water. We attribute this dewetting process of the oil layer from the microgel to the varying interfacial tension among the fluids consisting of the double emulsions when they are suspended in DI water (without surfactant); the absence of surfactants causes the destabilization of the oil layer, allowing easy separation of oil layer and thus facilitating collection of resulting microgel without extra washing procedure (Choi et al., 2016). As
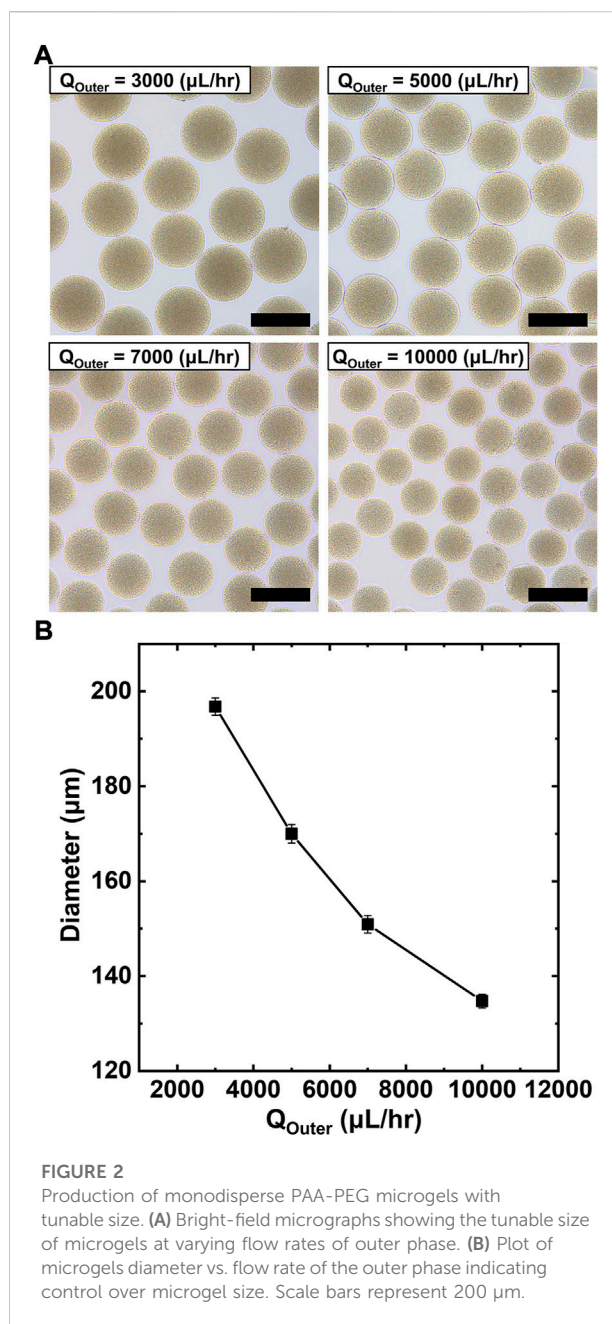
FIGURE 2
Production of monodisperse PAA-PEG microgels with tunable size. **(A)** Bright-field micrographs showing the tunable size of microgels at varying flow rates of outer phase. **(B)** Plot of microgels diameter vs. flow rate of the outer phase indicating control over microgel size. Scale bars represent 200 μm.

shown in Figure 1B, this microfluidic approach yields exceedingly uniform PAA-PEG microgels in a high throughput manner (i.e., about 400 spheres/s). The resulting PAA-PEG microgels are uniform, as shown in the bright-field micrograph of Figure 1C. We note that the PAA-PEG microgel's darkening is attributed to the presence of PAA with a large molecular weight (4,000,000 Da) due to light scattering, unlike bare PEG microgel. Size analysis of the microgels in Figure 1D shows a coefficient of variation (CV) of 0.78%, indicating that this approach enables simple

FIGURE 3
Flow patterns formed in the microfluidic device. **(A)** Phase diagram showing flow behavior as a function of flow rate of the prepolymer solution for inner core (Q_{inner}, y axis) and flow rates of the hexadecane for the sacrificial oil layer as a middle phase (Q_{middle}, x axis). **(B)** Bright-field micrographs showing **(a)** separated flow, **(b)** jetting, **(c)** uniform double emulsion, which are denoted as cross, open square, and solid circle, respectively. Scale bars represent 200 μm.

FIGURE 4
R-PE conjugation with PAA-PEG microgels. **(A)** Schematic of EDC/NHS reaction for R-PE conjugation with PAA-PEG microgels. **(B)** Fluorescence micrographs of R-PE conjugation with PAA-PEG microgels and negative controls. **(C)** Plot of normalized total fluorescence intensity for R-PE conjugation with PAA-PEG microgels and negative controls. **(D)** Fluorescence micrographs showing R-PE conjugation capability at varying PAA contents. **(E)** Plot of normalized total fluorescence intensity for dependence on PAA contents. Scale bars represent 200 μm.

and high-throughput production of highly uniform PAA-PEG microgels.

We can control the size of PAA-PEG microgels by simply tuning the flow rate, as shown in Figure 2. For instance, Figure 2A shows the resulting microgels prepared at varying flow rates of the outer phase. Specifically, Figure 2B shows that we can produce microgels with highly uniform diameters in 135–195 μm range simply by changing the flow rate of the aqueous outer phase (3,000–10000 μl/h). While increasing the viscosity of the prepolymer drop due to the addition of PAA, the as-prepared microgels at each flow rate condition are uniform. Compared to conventional single emulsion (i.e., water-in-oil
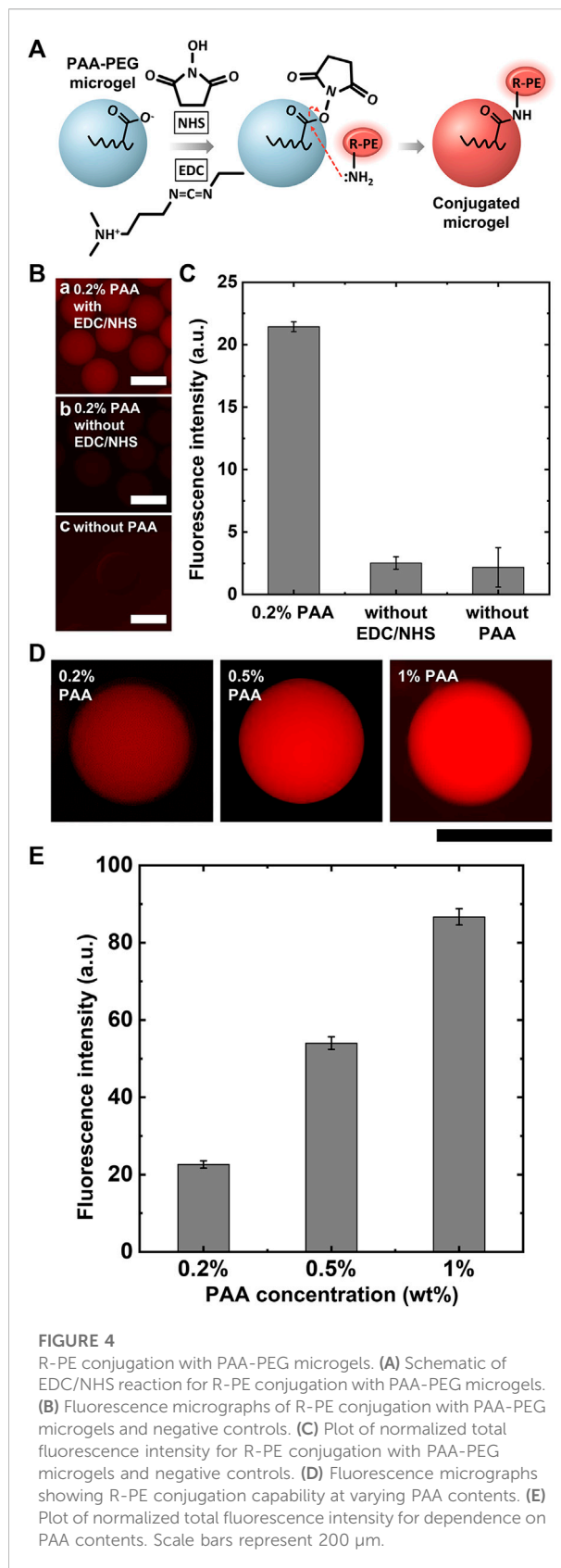
emulsion) based approaches, the proposed double emulsion (i.e., water-in-oil-in water) based routes are several advantages. First, we can create monodisperse carboxylate-functionalized microgels by simply incorporating PAA; while acrylic acid (AA) has been used in the previous report, (Liu et al., 2018) it is hard to achieve consistent functionalization due to AA's miscibility in oil. Second, this approach can produce microgels without additional washing step because the outer phase is an aqueous solution, which allows direct dispersion of the microgels followed by spontaneous dewetting of the oil shell. Lastly, we can minimize the volume of the immiscible oil phase to generate prepolymer drops, making the process simple and cost-efficient. In short summary, Figures 1, 2 demonstrate a high-throughput route for manufacturing of microgels with controllable dimensions.

We investigate the flow patterns as a function of the flow rates of each fluid used for the double emulsion drops. The phase diagram in Figure 3A shows representative patterns of the multiphasic flow in the capillary-based microfluidic device: (a) separated flow, (b) jetting, and (c) uniform double emulsion. The y-axis represents the flow rate of the prepolymer solution consisting of 10% PEGDA and 0.2% PAA for the inner core (Q_{inner}), while the x-axis represents the flow rates of the hexadecane oil for middle phase (Q_{middle}), which are supplied through the injection capillary. The aqueous outer phase (Q_{outer}) is maintained at a fixed flow rate (5,000 µl/h).

For high Q_{inner}, double emulsion drop does not occur at any given Q_{middle} because the flow rate of the middle phase cannot surround the inner core, which prevents drop generation (cross). For slightly lower Q_{inner}, the middle phase can fully surround the inner core due to relative high flow rate ratio of Q_{middle}/Q_{inner}, leading to drop formation in a jetting mode (open square); however, the controllable range in diameter is limited. As Q_{inner} is further reduced, the fluid thread breaks into drop in a dripping mode, producing monodisperse double emulsion with a thin oil layer (solid circles). The drop generation in this mode facilitates tuning of the double emulsion drop in diameter. The possible domains for uniform double drop become smaller by an increase in Q_{middle}. This result indicates that the hydrodynamic condition of each phase is crucial to the manufacturing of double emulsion formation. Overall, the flow rate dependence on drop formation shown in the phase diagram of Figure 3 provides windows of controllable parameters for simple and reliable manufacturing of double emulsion as a template for microgels.

Next, to investigate the capability of microgels for biofunctionalization, we examined protein conjugation with PAA-PEG microgels using a model protein R-phycoerythrin (R-PE) via a conjugation reaction scheme. We used the EDC/NHS chemistry (Figure 4A) to covalently couple the carboxylates in the PAA-PEG microgels with the primary amines of the R-PEs. We performed the conjugation reactions for 24 h and at a fixed R-PE concentration (2 µM) for this reaction scheme. As shown in the fluorescence micrographs of Figure 4B-a, PAA-PEG

microgels exhibit bright and uniform fluorescence intensity upon R-PE conjugation, indicating that PAA-PEG microgels can be coupled with large proteins (D_h = 11 nm) (Goulian and Simon, 2000; Contreras-Martel et al., 2001; Jung and Yi, 2015). PAA with large molecular weight has negligible loss due to immiscibility in oil phase, while AA is miscible with oil, resulting in non-uniform carboxylate functionality and showing inconsistent fluorescence intensity of R-PE, as shown in Supplementary Figure S1. We expect that the protein conjugation occurs on the whole of the microgel because the pore size of the particles consisting of 10% PEGDA is larger than that of R-PE (hydrodynamic diameter: 11 nm), which has been experimentally shown previously (Liu et al., 2018); the R-PE protein can penetrate through the microgel network consisting of 10% PEGDA and even more crosslinked microgel network consisting of 30% PEGDA. In contrast, microgels without EDC/NHS chemistry or PAA show minimal fluorescence when reacted with R-PE, as shown in Figure 4B-b,c; this result implies that PAA-PEG microgels have minimal non-specific adsorption with R-PE, due to inherent non-fouling property of PEG and PAA. We confirm that the fluorescence of the PAA-PEG microgels results from the acyl substitution of NHS ester-activated PAA-PEG microgels with the primary amines on R-PE. Capability to protein conjugation can be readily enhanced by increasing PAA concentration, as shown in Figures 4C,D. Figure 4E also shows consistent protein conjugation efficiency at varying PAA concentrations, evidenced by small error bars. These results in Figure 4 demonstrate that PAA-PEG microgels enable selective conjugation of large model protein via a simple conjugation scheme in a highly efficient manner.

Conclusion

We presented a capillary-based microfluidic approach to produce PAA-PEG microgels for efficient biomolecular conjugation. Unlike conventional microfluidic routes, this approach used double emulsion drops with a thin oil layer as templates, allowing production of monodisperse carboxylate functionalized microgels with minimal use of oil in a cost-efficient manner. By taking advantage of microfluidics, microgel's dimension can be tuned by simply varying flow rate of each phase. We established a phase diagram representing the operating flow conditions for uniform double emulsion drop formation, demonstrating a simple yet powerful approach to control complex fluids for creating functional microgels. Finally, we demonstrated that the resulting PAA-PEG microgels are used for efficient biomolecular conjugation, which is evidenced by uniform fluorescence intensity of R-PE protein unlike AA-PEG microgel. Overall, these results show the significant potential of the proposed microfluidic approach for production of functional microgels for broad applications in biosensor, cosmetics, and catalysis.

Data availability statement

The original contributions presented in the study are included in the article/Supplementary Material, further inquiries can be directed to the corresponding author.

Author contributions

YC, C-HC, and S-JL contributed to the conception and design of the study. YC and S-RP organized the database. YC performed the statistical analysis. YC and C-HC wrote the first draft of the manuscript. YC and C-HC wrote sections of the manuscript. All authors contributed to manuscript revision, read, and approved the submitted version.

Acknowledgments

Conflict of interest

The authors declare that the research was conducted in the absence of any commercial or financial relationships that could be construed as a potential conflict of interest.

Publisher's note

All claims expressed in this article are solely those of the authors and do not necessarily represent those of their affiliated organizations, or those of the publisher, the editors and the reviewers. Any product that may be evaluated in this article, or claim that may be made by its manufacturer, is not guaranteed or endorsed by the publisher.

Supplementary material

The Supplementary Material for this article can be found online at: https://www.frontiersin.org/articles/10.3389/fsens.2022.1016791/full#supplementary-material

References

Abdelaziz, H. M., Gaber, M., Abd-Elwakil, M. M., Mabrouk, M. T., Elgohary, M. M., Kamel, N. M., et al. (2018). Inhalable particulate drug delivery systems for lung cancer therapy: Nanoparticles, microparticles. *nanocomposites nanoaggregates* 269, 374–392. doi:10.1016/j.jconrel.2017.11.036

Choi, C. H., Jeong, J. M., Kang, S. M., Lee, C. S., and Lee, J. (2012). Synthesis of monodispersed microspheres from laplace pressure induced droplets in micromolds. *Adv. Mat.* 24 (37), 5078–5082. doi:10.1002/adma.201200843

Choi, C. H., Wang, H., Lee, H., Kim, J. H., Zhang, L., Mao, A., et al. (2016). One-step generation of cell-laden microgels using double emulsion drops with a sacrificial ultra-thin oil shell. *Lab. Chip* 16 (9), 1549–1555. doi:10.1039/C6LC00261G

Contreras-Martel, C., Martinez-Oyanedel, J., Bunster, M., Legrand, P., Piras, C., Vernede, X., et al. (2001). Crystallization and 2.2 Å resolution structure of R-phycoerythrin from gracilaria chilensis: A case of perfect hemihedral twinning. *Acta Crystallogr. D. Biol. Crystallogr.* 57 (1), 52–60. doi:10.1107/s0907444900015274

Daly, A. C., Riley, L., Segura, T., and Burdick, J. A. (2020). *Nat. Rev. Mat.* 5 (1), 20–43. doi:10.1038/s41578-019-0148-6

Dendukuri, D., and Doyle, P. S. (2009). The synthesis and assembly of polymeric microparticles using microfluidics. *Adv. Mat.* 21 (41), 4071–4086. doi:10.1002/adma.200803386

Dendukuri, D., Pregibon, D. C., Collins, J., Hatton, T. A., and Doyle, P. S. (2006). Continuous-flow lithography for high-throughput microparticle synthesis. *Nat. Mat.* 5 (5), 365–369. doi:10.1038/nmat1617

Goulian, M., and Simon, S. M. (2000). Tracking single proteins within cells. *Biophys. J.* 79 (4), 2188–2198. doi:10.1016/S0006-3495(00)76467-8

Hakala, T. A., Bialas, F., Toprakcioglu, Z., Bräuer, B., Baumann, K. N., Levin, A., et al. (2020). Continuous flow reactors from microfluidic compartmentalization of enzymes within inorganic microparticles. *ACS Appl. Mat. Interfaces* 12 (29), 32951–32960. doi:10.1021/acsami.0c09226

Hwang, E. T., and Lee, S. (2019). Multienzymatic cascade reactions via enzyme complex by immobilization. *ACS Catal.* 9 (5), 4402–4425. doi:10.1021/acscatal.8b04921

Jo, Y. K., and Lee, D. J. S. (2020). Biopolymer microparticles prepared by microfluidics for biomedical applications. *Small* 16 (9), 1903736. doi:10.1002/smll.201903736

Jung, S., and Yi, H. (2012). Fabrication of chitosan-poly (ethylene glycol) hybrid hydrogel microparticles via replica molding and its application toward facile conjugation of biomolecules. *Langmuir* 28 (49), 17061–17070. doi:10.1021/la303567p

Jung, S., and Yi, H. (2015). Facile micromolding-based fabrication of biopolymeric–synthetic hydrogel microspheres with controlled structures for improved protein conjugation. *Chem. Mat.* 27 (11), 3988–3998. doi:10.1021/acs.chemmater.5b00920

Lee, H. J., Roh, Y. H., Kim, H. U., Kim, S. M., and Bong, K. W. (2019). Multiplexed immunoassay using post-synthesis functionalized hydrogel microparticles. *Lab. Chip* 19 (1), 111–119. doi:10.1039/C8LC01160E

Leng, Y., Sun, K., Chen, X., and Li, W. J. (2015). Suspension arrays based on nanoparticle-encoded microspheres for high-throughput multiplexed detection. *Chem. Soc. Rev.* 44 (15), 5552–5595. doi:10.1039/C4CS00382A

Li, F., Lyu, D., Liu, S., and Guo, W. (2020). DNA hydrogels and microgels for biosensing and biomedical applications. *Adv. Mat.* 32 (3), 1806538. doi:10.1002/adma.201806538

Li, W., Zhang, L., Ge, X., Xu, B., Zhang, W., Qu, L., et al. (2018). Microfluidic fabrication of microparticles for biomedical applications. *Chem. Soc. Rev.* 47 (15), 5646–5683. doi:10.1039/C7CS00263G

Liang, Q., Bie, N., Yong, T., Tang, K., Shi, X., Wei, Z., et al. (2019). The softness of tumour-cell-derived microparticles regulates their drug-delivery efficiency. *Nat. Biomed. Eng.* 3 (9), 729–740. doi:10.1038/s41551-019-0405-4

Liu, E. Y., Jung, S., Weitz, D. A., Yi, H., and Choi, C. H. (2018). High-throughput double emulsion-based microfluidic production of hydrogel microspheres with tunable chemical functionalities toward biomolecular conjugation. *Lab. Chip* 18 (2), 323–334. doi:10.1039/C7LC01088E

Liu, E. Y., Jung, S., and Yi, H. (2016). Improved protein conjugation with uniform, macroporous poly(acrylamide-*co*-acrylic acid) hydrogel microspheres via EDC/NHS chemistry. *Langmuir* 32 (42), 11043–11054. doi:10.1021/acs.langmuir.6b02591

Qu, H., Yu, M., Du, W., Xu, L., Lyu, W., and Shen, F. (2019). Slip molding for precision fabrication of microparts. *Langmuir* 36 (2), 585–590. doi:10.1021/acs.langmuir.9b03156

Riley, L., Schirmer, L., and Segura, T. J. (2019). Granular hydrogels: Emergent properties of jammed hydrogel microparticles and their applications in tissue repair and regeneration. *Curr. Opin. Biotechnol.* 60, 1–8. doi:10.1016/j.copbio.2018.11.001

Steinacher, M., Cont, A., Du, H., Persat, A., and Amstad, E. (2021). Monodisperse selectively permeable hydrogel capsules made from single emulsion drops. *ACS Appl. Mat. Interfaces* 13 (13), 15601–15609. doi:10.1021/acsami.1c00230

Wang, W., Zhang, M. J., and Chu, L. Y. (2014). Functional polymeric microparticles engineered from controllable microfluidic emulsions. *Acc. Chem. Res.* 47 (2), 373–384. doi:10.1021/ar4001263

Yadavali, S., Jeong, H. H., Lee, D., and Issadore, D. (2018). Silicon and glass very large scale microfluidic droplet integration for terascale generation of polymer microparticles. *Nat. Commun.* 9 (1), 1222–1229. doi:10.1038/s41467-018-03515-2